

## ACOUSTICAL PROBLEMS IN HIGH ENERGY PULSED E-BEAM LASERS

T. E. Horton and K. F. Wylie  
University of Mississippi

### SUMMARY

During the pulsing of high energy, CO<sub>2</sub>, electron-beam (E-beam) lasers, a significant fraction of input energy ultimately appears as acoustical disturbances. The magnitudes of these disturbances are quantified by computer analysis. Acoustical and shock impedance data are presented on materials (Rayleigh type) which show promise in controlling acoustical disturbance in E-beam systems.

### INTRODUCTION

The repetitively pulsed electron-beam (E-beam) laser, figure 1, has proven to be an efficient and compact means of achieving high power levels in CO<sub>2</sub> at atmospheric pressure, (ref. 1, 2, 3). In such a system the E-beam supplies high energy primary electrons which through secondaries produce a plasma in the laser cavity for a period  $\tau_p$ , the time the gun is pulsed on. A sustainer voltage applied across the plasma supplies the energy for excitation of the laser states. By adjusting the sustainer field strength, the pumping of the laser state is optimized. As the lasing pulse duration approaches  $\tau_1$  (the relaxation time of the lower lasing state) optimum lasing output is achieved. For pulses less than  $\tau_1$  the lasing process is self-terminated by the incapacity of the lower state to relax; while for longer pulses the lower state capacity is reduced by gas heating. Practical values of  $\tau_1$  range from 1 to 10  $\mu$ sec and are dependent upon gas composition and temperature. For the 1:2:3 (CO<sub>2</sub>:N<sub>2</sub>:He) mixture at 300 K considered in this work the value is 5  $\mu$ sec.

In pulsed operation the sudden and sometimes nonuniform deposition of energy in the excited states of the laser media leads through vibrational energy cascading to pressure and temperature gradients which drive acoustical disturbances (ref. 4, 5, 6). Clearly, for efficient operation, these acoustical disturbances must be controlled since nonuniformity in the laser gas can lead to a reduction in beam quality and also to catastrophic arcing. To accommodate the heating of the laser gas, one must either execute a pulsed duty cycle of sufficient duration to allow dissipation of the energy or remove the energy from the cavity by flowing the gas through the cavity. The changes in gas properties and velocities which result from forced mass transport through the laser cavity and from heating the laser cavity have been designated as aero-acoustical effects.

The purpose of the present investigation is to quantify these effects and suggest promising means of controlling them. Constraints considered were

(1) power inputs up to 500 joules/liter of cavity gas, (2) laser cavity gas initially at standard temperature and pressure and composed of a 1:2:3 molar mixture of carbon dioxide, nitrogen, and helium, (3) the laser cavity has a 200-cm dimension along the optical axis, a 15-cm dimension between anode and cathode, and the discharge is considered to be 15 cm wide.

The first section of this paper delineates the magnitude of the problem created by bulk heating of the laser gas. The problem posed by nonuniform heating within the laser cavity, cathode waves, et al, have been treated in references 4, 5, and 6 and are not considered in this work. The second section treats the control of the discharge shocks by multiple reflection from low-pressure-drop, porous absorbers mounted in planes normal to the flow axis. In particular, the measured properties of Rayleigh materials, absorbers composed of thin walled tubers or honeycomb, are present in this second section. The paper concludes with a discussion of the feasibility of using the Rayleigh materials in a multiple reflection application.

#### MAGNITUDES FOR ACOUSTICAL DISTURBANCES

For optimum pulsed performance, the volumetric heating of the laser gas occurs by two relaxation paths. Initially during lasing, the rapid relaxation through the lower laser level results in a small temperature rise. The magnitude and time scale of this rise are insignificant acoustically. The primary heating takes place after lasing as the major fraction of the pumped energy cascades out of the upper states over the comparatively long period  $\tau_u$ , the relaxation time of the upper laser level -- 60  $\mu$ sec. Thus the acoustically significant temperature rise occurs on a time scale which is long for optimum lasing but which is short for significant changes in liter size systems. This justifies the assumption of constant volume heating of the gas in the laser cavity. These changes within the laser cavity lead to the formation of expansion and compression waves which are the source of acoustical problems in subsequent pulses.

For modeling the performance of an E-beam system, a computer program is desirable which, from a gasdynamic point of view, satisfies the coupled state, continuity, momentum, energy, and kinetic rate equations as a function of time over a three-dimensional array of points which includes the laser cavity and adjacent gas. When the gas is confined between two electrodes, as it is along the E-beam axis, and when some of the dimensions such as the optical axis are an order of magnitude or more greater than the other significant dimensions, then a one-dimension solution is a meaningful first approximation. Furthermore, with the short pulse condition argued above, the laser kinetics may be rationalized to be decoupled from the gasdynamic. The gasdynamics behavior is thus coupled to the kinetics in such a way that the problem can be posed as one of satisfying the one-dimensional mass, momentum, and energy conservation equations subject to a laser cavity heating rate predicted by constant volume laser code of reference 1.

A computer code incorporating the above assumptions is described in reference 7 and has been exercised to generate the results given below. Computations have been performed for a 1:2:3 mixture at power inputs ranging from 200 joules/liter to 500 joules/liter for beam turn-on times of 2  $\mu$ sec and 10  $\mu$ sec. For a 400-joule/liter input, the development of the compressive shock and expansion wave are illustrated over a 380- $\mu$ sec interval in figure 2. Shortly after 140  $\mu$ sec, the expansion wave will be reflected from the plane at the E-beam center, and a reduced density wave will propagate back through the 7.5-cm dimension of the discharge. The density minimum for the range of power inputs considered occurs at between 200 and 220  $\mu$ sec. The variation of the minimum density in the reflected expansion wave with power input is illustrated in figure 3. These waves determine arcing limits for the sustainer field. For the energy inputs considered, the compressive waves were equivalent to the following Mach number shocks in air:

Energy Input (joules/liter)	Shock Mach Number	$\frac{\Delta P}{P}$
500	1.35	.960
400	1.28	.745
300	1.22	.570
200	1.15	.376

The strength of these shocks are far greater than the usual disturbances encountered in acoustics, with the equivalent sound intensities of 100 watts/cm<sup>2</sup> and 1000 watts/cm<sup>2</sup> for the 200-joule/liter and 500-joule/liter energy loadings. Thus the shocks listed above fall in the 180-to 190-db intensity range -- 40 to 50 db above the threshold of pain and 110 to 120 db above the normal speech level.

Another way to put the magnitude of the "acoustical problem" is to consider the amount of the energy input which is deposited in the adjacent gas as the laser cavity gas expands. A simple analysis based on constant volume heating with subsequent isentropic expansion back to atmospheric pressure yields the results given in figure 4. Clearly about one third of the energy input goes into "acoustical energy" while typically only 10% of the input goes into lasing.

#### ATTENUATOR CONCEPT AND MATERIALS

The problem is controlling disturbances of the magnitude discussed above in interpulse times at 10 to 100  $\mu$ sec without causing excessive pressure drop in the flow. The concept considered is to dissipate the acoustical energy in multiple reflections from porous materials located on planes parallel to the E-beam axis and optical axis in close proximity to the discharge.

The intent below is to examine the properties of porous materials for this application. The properties of interest are the reflection coefficient and the attenuation coefficient. These properties are functions of the permeability and porosity of the material. The reflection coefficient is a strong function of the

frontal porosity. A high permeability is desired to reduce the steady flow pressure drop, but this means a reduced attenuation coefficient. Clearly what is desired is sufficient porosity to give rise to reflections of significant fractions of the acoustical energy with sufficient permeability and length to fully dissipate the energy ingested by the absorber.

The data of references 8, 9, 10, and 11 indicate that Rayleigh type materials may be ideally suited as acoustical absorbers for shocks. Three types of Rayleigh materials were used in this investigation. All were 7.5 cm long and made from Therma Comb ceramic. The size and corrugation geometries are shown in figure 5. For identification these have been referred to as fine, medium, and coarse.

For the data reported below the materials were mounted in a 7.5-cm diameter shock tube with the driver at atmospheric pressure. The small amplitude properties of the materials were determined by transmission-line standing-wave-ratio tests. For these measures the shock tube was fashioned into an acoustic transmission line with terminators of known impedance so that infinite thickness (front surface reflection only) impedances,  $W/pc$ , could be determined. The value for  $W$  found in this manner were real ( $\theta_{\max} = \pm 10^0$ ) and frequency independent ( $\pm 10\%$ ). Typical values  $W/pc$  were 2.2 for the fine, 1.5 for the medium, and 1.3 for the coarse. Thus, for semi-infinite layers, the  $R_p^2$  values would be 0.14, 0.04, and 0.017, respectively. Based upon Rayleigh's theory for impedance of small pipes, the reflectivity  $R_p$  is a function of the porosity  $\sigma$ . The values for  $R_p$  yield porosities of 0.45 for the fine, 0.67 for the medium and 0.77 for the coarse. These values are indicative of the flow areas to total area shown in figure 5.

Values of the attenuation constant  $\alpha$  obtained in these experiments are shown in figure 6. The attenuation constant should correlate with the steady flow pressure drops. When the measured static flow resistivities of 5150, 2470, and 717 mks rayls/m (fine, medium, and coarse) are corrected to a common velocity base by multiplying by the porosity, they are in the ratio of 4.3:3.0:1.0. Similarly at 100 Hz the attenuation constants are in the ratio 4.0:2.7:1. The Rayleigh materials considered in this investigation all have acoustical properties which are of the same order of magnitude as those of the foametals which have previously been considered as shock absorbers (ref. 8).

Using the shock tube in its intended configuration, a series of tests were run on Rayleigh materials with velocities and pressure amplitudes of both reflected and transmitted waves being observed. As shown in figure 7, the reflected wave velocities for the medium Rayleigh materials are comparable to the foamental data of ref. 8. The results of the series of tests are depicted in figure 8 as the double cross-hatched area with extrapolation depicted by single cross-hatching. Here  $P_2$  is the pressure behind the incident wave and  $\Delta P$  is the pressure difference between the reflected and incident waves. In addition to tests on the Rayleigh type attenuators, a limited number of tests were made on stainless steel screens, 0-grade steel wool, and polyurethane foam. The tests on the foam and steel wool were not pursued because of adverse characteristics of these materials. The steel wool attenuator failed to transmit the

wave significantly but was deemed impractical, since after each shock small fragments of steel wool were found in the tube. The reflected wave properties of the steel wool (7 rolls compacted in a cylinder 14 cm long and 7.5 cm in diameter) were similar to foametal and hexcell ceramics as shown in figure 7. Screens appear to be quite promising materials from our limited testing. Screens can be easily stacked or tailored to achieve a prescribed set of properties.

### CONCLUSIONS

The cogent question is: Can Rayleigh or other shock attenuators mounted in the flow of an E-beam system achieve reduction of shock and acoustical disturbances to sufficient amplitudes to assure good beam quality in repetitively pulsed operations? A conclusive answer to this question can be made by using the attenuator data of this study in a comprehensive analysis of a system taking into account reflection of waves back into the system after transmission through the attenuators. However, if these waves which are reflected back into the system are neglected, one finds that damping of Mach 1.35 waves to less than 1/10 their original value can be easily achieved in 4 reflections. This is a 20-db reduction and a reduction to small amplitude waves. A further 43-db reduction in 5 reverberations can be achieved if the fine Rayleigh material ( $R_p^2 = 0.14$ ) is used. This 63-db reduction of a 500-joule/liter pulse in less than 10 reverberations is the order of reduction desired.

Further support for the use of the flow axis attenuation concepts is achieved by a comparison of the pressure traces in figure 9. In figure 9a the successive reflection of an initial Mach 1.35 pressure wave from the driver end of a shock tube is depicted. In figure 9b the 7.5-cm length of the fine Rayleigh material has been inserted 90 cm from the pressure gage. The damping of both the 5-msec reflected wave and the 12- to 20-msec retransmitted wave is quite dramatic. The 90-cm distance between the absorber and backplate of the driver and overall 3.3-m length of the system dictates a time scale which is far larger than that of the shorter E-beam flow axis dimensions.

## REFERENCES

1. Kast, S. and Cason, C.: Performance Comparison of Pulsed Discharge and E-Beam Controlled CO<sub>2</sub> Lasers. J. Appl. Phys., Vol. 44, 1973, p. 1631.
2. Cason, C.: Review of CO<sub>2</sub> E-Beam Laser Operation and Heat Transfer Problems. AIAA Paper No. 74-686, AIAA/ASME Thermophysics and Heat Transfer Conference, Boston, MA, 1974.
3. Basov, N. G.; Danilychev, V. A.; et al.: Maximum Output Energy of an Electron-Beam-Controlled CO<sub>2</sub> Laser. Sov. J. Quantum Electronics, Vol. 4, 1975, p. 1414.
4. Pugh, E. R.; Wallace, J.; Jacob, J. H.; Northam, D. B.; and Daugherty, J. D. Optical Quality of Pulsed Electron-Beam Sustained Lasers. Appl. Optics, Vol. 13, 1974, p. 251.
5. McAllister, G. L.; Draggoo, V. G.; and Eguchi, R. G.: Acoustical Wave Effects on the Beam Quality of a High Energy CO Electric Discharge Laser. Appl. Optics, Vol. 14, 1975, p. 1290.
6. Culick, F. E. C.; Shen, P. I.; and Griffins, W. S.: Acoustical Waves Formed in an Electric Discharge CO Laser Cavity. AIAA Paper No. 75-851, 1975.
7. Horton, T. E.; Wylie, K. F.; Wang, S. Y.; and Rao, M. S.: Modeling the Acoustical Performance of E-Beam Systems, Oct. 1976.
8. Beavers, G. S. and Matta, R. K.: Reflection of Weak Shock Waves from Permeable Materials. AIAA J., Vol. 10, 1972, p. 959.
9. Schlemm, H.: Über das Reflexionsverhalten Schwacher Stosswellen an Akustischen Absorben in Luft. Acustica, Vol. 13, 1963, p. 302.
10. Meyer, E. and Reipka, R.: Das Reflexions- und Durchlassverhalten von Stosswellen and porösen Absorben. Acustica, Vol. 16, 1965/66, p. 149.
11. Reipka, R.: Die Ausbreitung von Stosswellen in verengten Kanälen. Acustica, Vol. 19, 1967/68, p. 271.

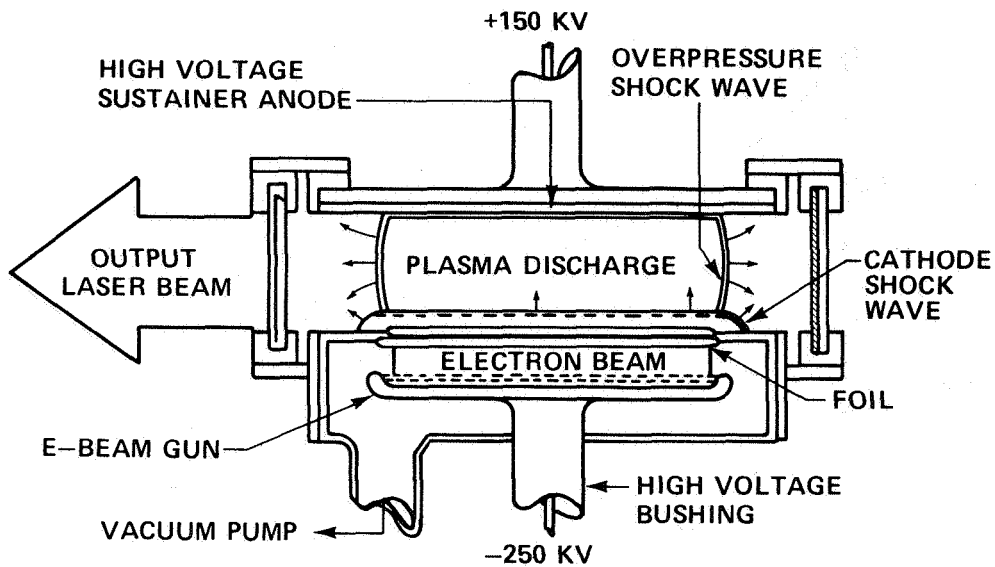


Figure 1.- Schematic views in optical and E-beam plane of an electron-beam laser. Overpressure waves typical of pulsed operation are shown.

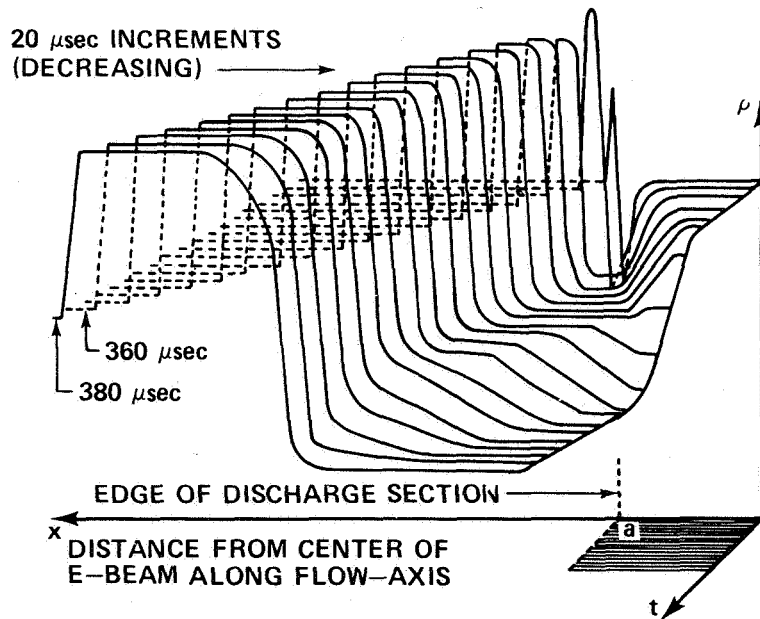


Figure 2.- Density variation at 20  $\mu\text{sec}$  intervals for a 1:2:3 mixture and a power input of 400 J/liter. The expansion and compression waves start at the edge of the discharge ( $x = a$ ). The expansion wave propagates to the E-beam center plane ( $x = 0$ ) where it is reflected and propagates back through the discharge.

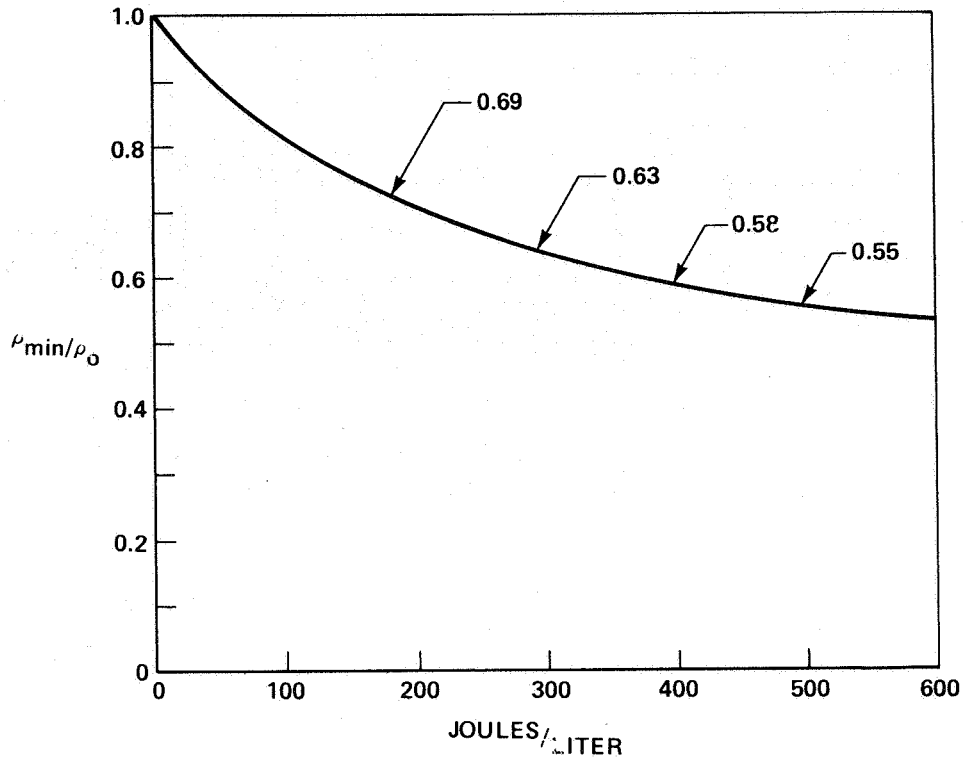


Figure 3.- Dependence of minimum density achieved at E-beam center plane on power input. The power input pulse length was 2  $\mu$ sec. The mixture was 1:2:3.

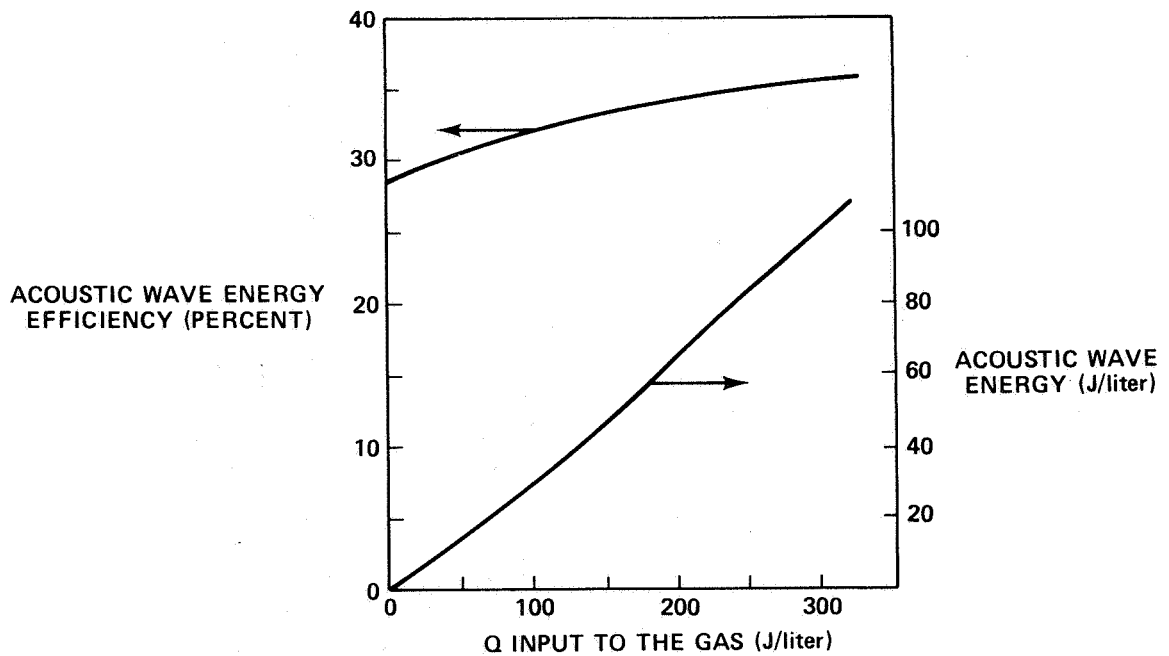


Figure 4.- Acoustical wave energy and conversion efficiency for a 1:2:3 mixture with 10% laser efficiency.

THE MATERIALS ARE IDENTIFIED FROM LEFT TO RIGHT AS FINE, MEDIUM, AND COARSE. THE TRANSVERSE FLOW RESISTIVITIES ARE 5.15, 2.47, AND 0.717 rayl/cm, RESPECTIVELY.

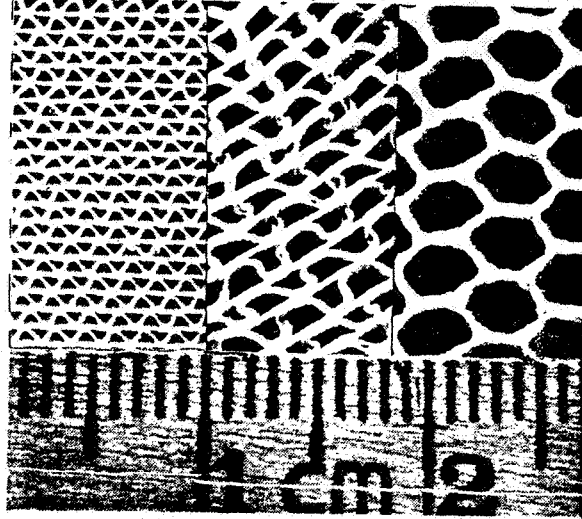


Figure 5.- Rayleigh absorber materials.

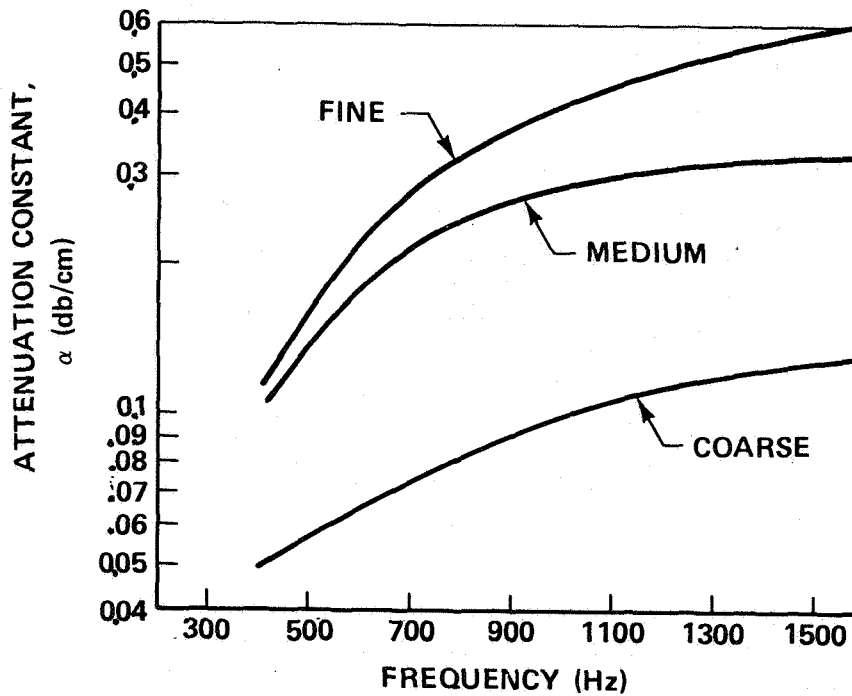


Figure 6.- Attenuation constant vs frequency for the three Rayleigh materials.

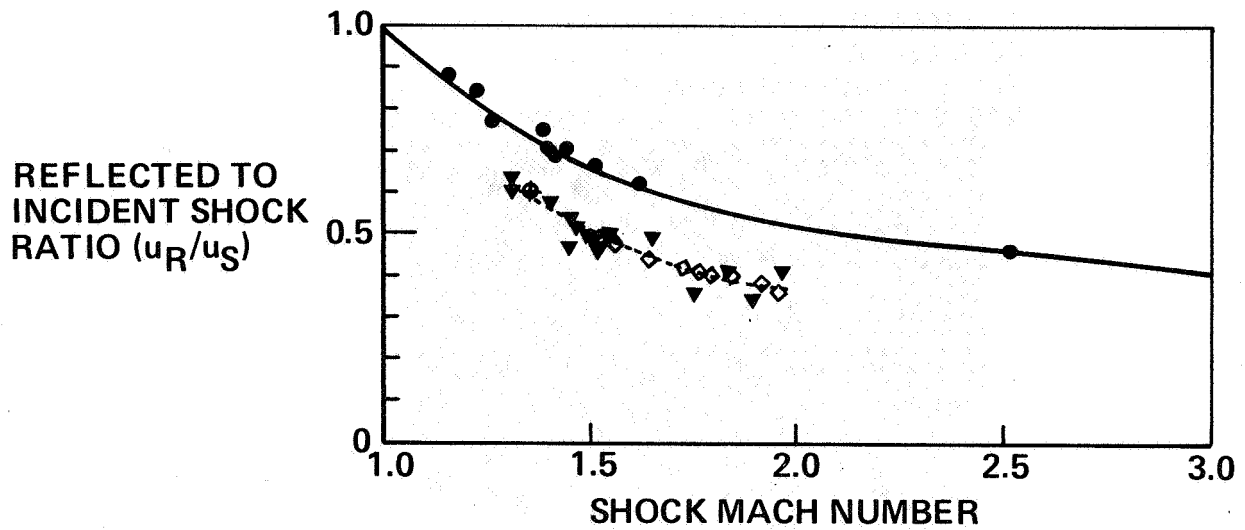


Figure 7.- Dependence of reflected shock velocity on incident shock Mach number. ● Solid boundary reflection, ▼ medium Rayleigh material, ◊ steel wool between screens, ◊ foametal (ref. 8).

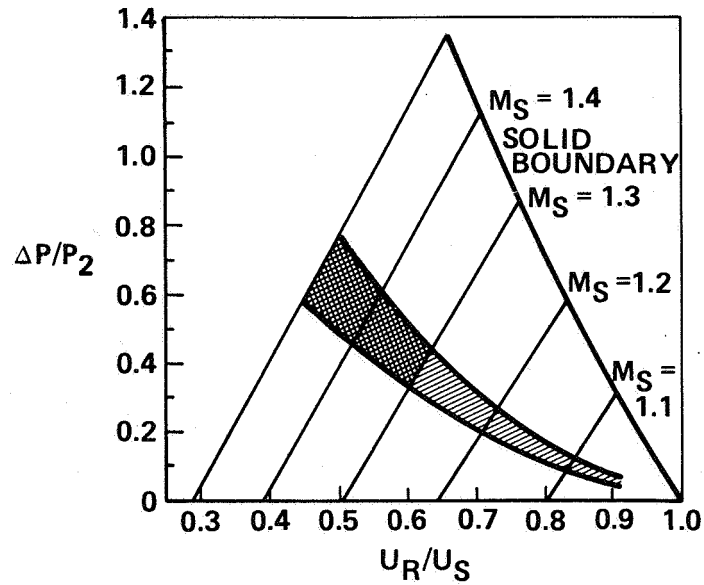
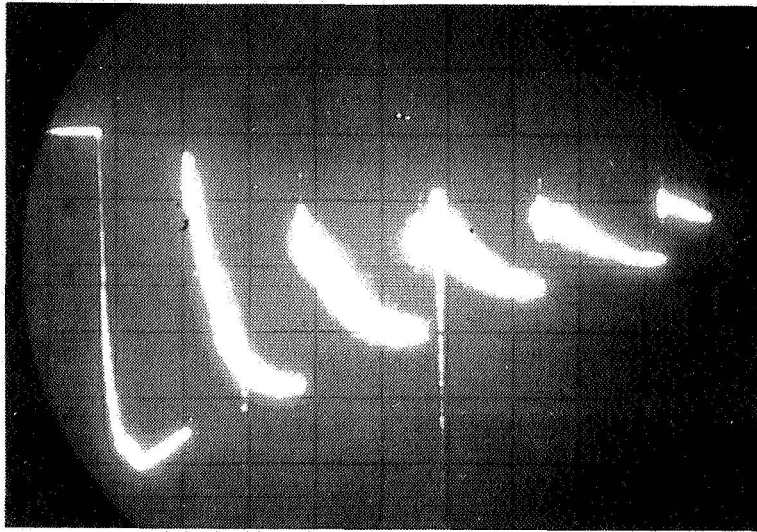
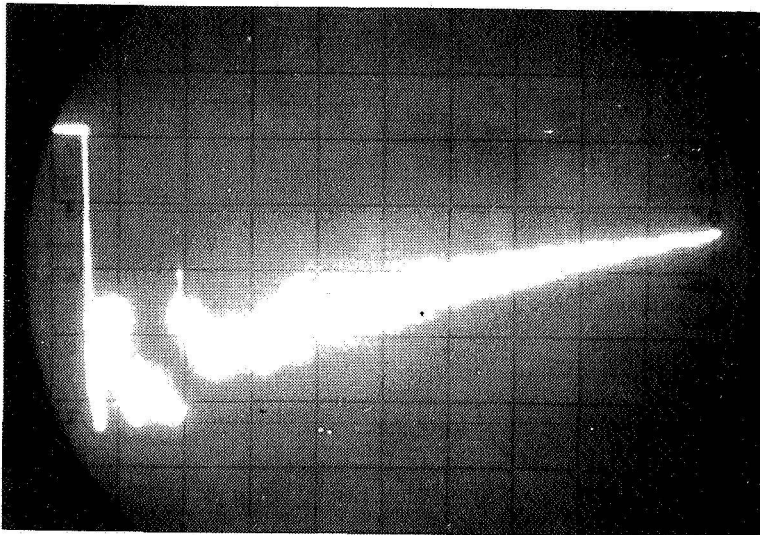


Figure 8.- Shock wave reflection properties. The dependence of reflected shock waves on incident Mach number is shown for attenuator materials listed in figure 7. The normalized reflected pressure increase,  $\Delta P/P_2$ , is shown as a function of normalized shock wave velocity.



(a) Without attenuator.



(b) With a 3-in. thickness of the "fine" Rayleigh attenuator located 8 in. from the driver diaphragm and 3 ft from the endplate pressure transducer.

Figure 9.- Pressure history at the driver endplate of a 11-ft closed shock tube with an initial shock of Mach number of 1.35 into air at standard temperature and pressure. Time base 10 msec/div.